

CrystEngComm

Accepted Manuscript



This is an *Accepted Manuscript*, which has been through the Royal Society of Chemistry peer review process and has been accepted for publication.

Accepted Manuscripts are published online shortly after acceptance, before technical editing, formatting and proof reading. Using this free service, authors can make their results available to the community, in citable form, before we publish the edited article. We will replace this *Accepted Manuscript* with the edited and formatted *Advance Article* as soon as it is available.

You can find more information about *Accepted Manuscripts* in the [Information for Authors](#).

Please note that technical editing may introduce minor changes to the text and/or graphics, which may alter content. The journal's standard [Terms & Conditions](#) and the [Ethical guidelines](#) still apply. In no event shall the Royal Society of Chemistry be held responsible for any errors or omissions in this *Accepted Manuscript* or any consequences arising from the use of any information it contains.



The Pivotal Role of Oxygen Interstitials in the Dynamics of Growth and Movement of Germanium Nanocrystallites

K. H. Chen,^a C. C. Wang,^a W. T. Lai,^{a,b} T. George^a and P. W. Li^{*a,b}

Received 00th January 20xx,
Accepted 00th January 20xx

www.rsc.org/

We report an unusual “symbiotic” behavior of oxygen interstitials acting in concert with Ge and Si interstitials at high temperature inducing morphology changes and autonomous migration of Ge nanocrystallites within SiO₂/Si₃N₄ layers. The Ge nanocrystallites were originally generated by the selective oxidation of SiGe nano-pillars grown and lithographically patterned over buffer Si₃N₄ layers on Si substrates. The coalescence and movement of these Ge nanocrystallites appear to be very sensitive to the presence and the flux of oxygen interstitials especially at the Ge nanocrystallites/buffer Si₃N₄ interface. A range of different morphologies are observed for Ge nanocrystallites that are directly attributable to the influence of oxygen interstitial concentration and consequently the interstitial Si and Ge concentrations. In combination with Si and Ge interstitials, oxygen interstitials activate the coalescence of sparsely-distributed Ge nanocrystallites and concurrently their migration towards the source of Si interstitials, i.e. the buffer Si₃N₄ layers, through a catalytically-enhanced local decomposition and subsequent oxidation of both the SiO₂ and Si₃N₄ buffer layers. We also show that these symbiotic effects are “tunable” by increasing the Ge content of the SiGe nano-pillars. Dense distributions of Ge nanocrystallites generated from high Ge content SiGe nano-pillars remain static and show no changes in their morphology possibly because oxygen interstitials are simply unable to penetrate these clusters and consequently unable to induce symbiotic Si and Ge interstitial generation.

Introduction

Semiconductor nanodots have aroused extensive interest in recent years for their great versatility and functionality enabling diverse device applications.^{1,2} The key challenge for the production of these mostly self-assembled nanostructures is to achieve precise control over the placement, structure and properties of individual nanodots as well as the materials within which they are embedded. Significant efforts³⁻⁹ have been made to understand the mechanisms behind the growth of the nanodots in order to control critical parameters such as shape, size, chemical composition, spatial location, and the embedment environments. These parameters significantly influence not only their electronic structures and optical properties but also the methods for contacting or communicating with the nanodots. Detailed knowledge and understanding of how the nanodots are created, and especially their interactions with their local environments are therefore crucial to achieve a high level of nanofabrication control of an otherwise random growth process. In previous reports,¹⁰⁻¹³ we have described successful demonstrations of CMOS-compatible, hybrid, lithographically-patterned/self-assembled approaches to not only deliberately grow spherical Ge nanodots of variable sizes, but also to control their spatial locations

within dielectric layers such as Si₃N₄ and SiO₂. These “designer” Ge nanodots are generated using the exquisite control available through selective oxidation of poly-Si_{1-x}Ge_x nanopatterned-pillars grown over buffer layers of Si₃N₄ on Si substrates. An intriguing discovery, previously made by us¹⁰⁻¹³ is that for a given Ge content within the poly-Si_{1-x}Ge_x nano-pillars, high-temperature thermal oxidation results in the consolidation of segregated, irregularly-shaped Ge nanocrystallites within each pillar into fully-coalesced, spherical Ge dots, which also exhibit controllable migration through the underlying buffer Si₃N₄ layer.

Such an unusual Ostwald ripening behavior coupled with autonomous migration of the Ge nanocrystallites embedded within newly-formed SiO₂ matrices was shown to be enabled by means of a complex, cooperative mechanism that involves the interplay of Ge, Si, and oxygen interstitials.¹¹⁻¹³ Previously, we have reported, in detail, the roles of Ge and Si interstitials in facilitating this unique mechanism.¹²⁻¹³ In this work, we further examine the role of oxygen interstitials acting in concert with Ge and Si interstitials to facilitate the growth and migration of the Ge nanocrystallites.

Experiments

^a Department of Electrical Engineering and Center for Nano Science and Technology, National Central University, ChungLi, Taiwan, 32001, Republic of China.

^b Department of Electronics Engineering, National Chia Tung University, Hsinchu, Taiwan, 300, Republic of China. Email: pwli@ee.nctu.edu.tw

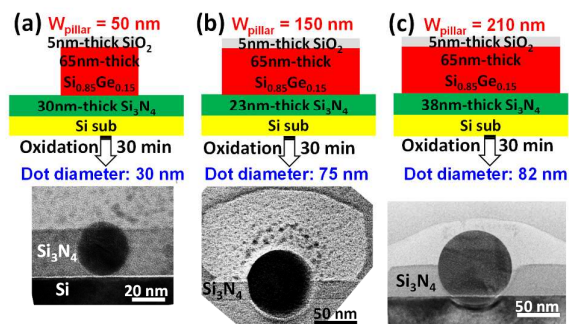


Fig. 1 Demonstration of control of size, location and morphology for Ge nanodots. Poly-Si_{0.85}Ge_{0.15} nano-pillars originally grown and lithographically patterned over buffer layers of Si₃N₄ with varying widths of (a) 50nm, (b) 150nm, and (c) 210nm were oxidized at 900°C for 30 min in an H₂O ambient. Transmission electron micrographs (TEMs) below show the resulting Ge spherical nanodots that have migrated and become embedded within the Si₃N₄ buffer layer. Note that the magnification is intentionally decreased in the micrographs for (b) and (c) in order to accommodate the larger Ge nanodot sizes.

As reported previously,^{11–14} Ge nanodots catalyze the decomposition of both of the surrounding SiO₂ and Si₃N₄ matrices. In brief, during the high-temperature oxidation of the poly-Si_{1-x}Ge_x nanopillars originally grown and lithographically patterned over buffer layers of Si₃N₄, the Si content of these nanopillars is preferentially oxidized. The remaining Ge content within each poly-SiGe grain is squeezed radially inwards towards the core of the oxidized pillar, resulting in a cluster of Ge nanocrystallites surrounded by the newly-formed SiO₂ matrix. Further thermal oxidation results in the consolidation via Ostwald Ripening¹⁵ of the growing Ge nanocrystallites within each pillar accompanied by concurrent, controllable migration through both the SiO₂ matrix and the underlying buffer Si₃N₄ layer (Figure 1(a)–(c)). We have previously shown^{10,13,14} that this “burrowing” action occurs via the Ge nanocrystallites catalytically-enhancing local oxidation of the Si₃N₄ buffer layer. The Si₃N₄ dissociates to release a high flux of Si interstitials that subsequently migrate through the SiO₂ matrix to the surface of the Ge nanocrystallites and consequently decompose the surrounding oxide via the reaction of Si + SiO₂(s) → 2SiO(g).¹⁶ The escape of SiO leads to void formation in the direction of increasing Si interstitial concentration, and thereby allows the Ge nanocrystallites not only to expand via the acquisition of Ge interstitials (Ostwald Ripening), but also enables the migration of the Ge nanocrystallites towards the source of Si interstitials, i.e. the underlying Si₃N₄ buffer layer. The SiO-enabled void formation mechanism also releases the interfacial stress between the growing Ge nanocrystallites and the surrounding SiO₂ matrix, ultimately transforming the morphology of the fully-coalesced Ge nanodot into a surface-stress-free spherical shape.¹⁷

As observed in the micrographs in Figure 1, as the Ge nanodot migrates, the SiO₂ “re-forms” behind the dot.^{10–14} The

explanation for the oxide re-formation on the distal end of the Ge nanodots is that both Si interstitials and the previously-generated SiO migrate along the surface of the Ge nanodots to be oxidized by oxygen interstitials migrating from the nanopillar surfaces exposed to the ambient oxidation furnace atmosphere. Thus, a SiO₂ destruction/construction mechanism dynamically occurs facilitating the growth and migration of the Ge nanodots.¹³ Deeper penetration of the Ge nanodot into the Si₃N₄ buffer layer occurs by a variant of the above mechanism whereby the Si₃N₄ oxidation is locally-enhanced ahead of the Ge nanodot, again re-forming SiO₂ behind the Ge nanodot during migration.¹⁴

This remarkable coarsening and migration behavior of Ge nanodots is the basis for our ability to produce precisely-located, size-tunable, spherical Ge dots by tailoring the Ge content of the original, lithographically-patterned poly-SiGe nano-pillars. The nanodot size itself is lithographically controllable via control of the geometrical dimensions (width and height) of the original Si_{1-x}Ge_x pillars prior to oxidation.¹⁸ Extensive cross-sectional transmission electron microscopy (CTEM) observations confirm that the thermal oxidation process converts 50–210nm-wide, 65±5nm-thick Si_{0.85}Ge_{0.15} nano-pillars to single spherical Ge dots per pillar ranging in diameter from 30–83nm (Figure 1(a)–(c)) with a good linear relationship between the volume of a spherical Ge dot and the total Ge content of the Si_{0.85}Ge_{0.15} pillar.

Results and discussions

Dramatic changes are observed in the morphology and migration behavior of the Ge nanodots (Figure 2) when the widths of the original Si_{0.85}Ge_{0.15} nanopillars exceed 300nm. For the case of the 305nm-wide Si_{0.85}Ge_{0.15} pillar following a

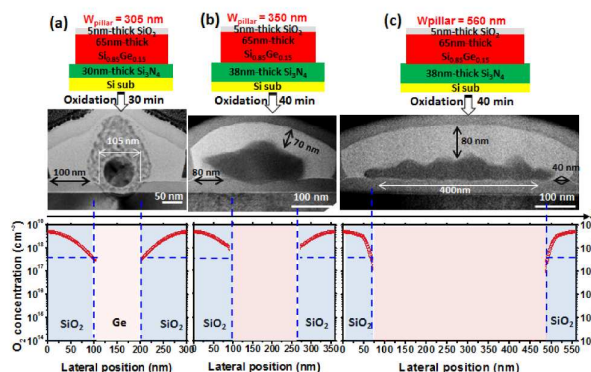


Fig. 2 Dramatic changes in Ge nano-crystallite morphology occur as the width of the Si_{0.85}Ge_{0.15} nano-pillars is increased to (a) 305nm, (b) 350nm, and (c) 560nm and subjected to the same oxidation conditions as above at 900°C for 30–40 min in an H₂O ambient. Starting from a spherical morphology observed for nanopillar widths around 305 nm, a range of different morphologies are observed that are directly attributable to the influence or lack thereof of the oxygen interstitial concentration which decreases by several orders of magnitude as the lateral size of the Ge nano-crystallite cluster increases to 500 nm.

30min, 900°C thermal oxidation, a very large spherical Ge nanodot of approximately 105nm in diameter is formed per pillar. However, during thermal oxidation the larger reaction surface area of the Ge nanodot leads to faster penetration through the entire thickness of the Si₃N₄ buffer layer and into the Si substrate. Once within the Si substrate, the much higher flux of Si interstitials generated from the Si substrate makes the Ge nanodot “explode”¹¹ due to the decoration of internal defects within the Ge nanodot by Si which subsequently forms oxide in situ and breaks up the Ge nanodot. Figure 2(a) shows an intact spherical Ge nanodot in the foreground and an exploded Ge nanodot from a different 305 nm-wide pillar in the background.

As the Si_{0.85}Ge_{0.15} nanopillar width is further increased to 350nm coalescence through Ostwald Ripening is no longer observed. As indicated by the concentration plots in Fig. 2, Oxygen interstitials are no longer able to penetrate the dense Ge nanocrystallite clusters and initiate the generation of Si interstitials by oxidizing the Si₃N₄ buffer layer. As a result, the Ge nanocrystallite clusters exhibit a flatter, “pancake” like morphology with occasional asperities within the cluster. Even though these Ge nanocrystallites exist in large quantity and are still in close contact with the Si₃N₄ buffer layer underneath, neither visible coalescence nor obvious cluster migration is observed (Figures 2(b) and (c)). It clearly appears that the previously-observed Ge catalyzed local oxidation of Si₃N₄¹⁰⁻¹⁴ is no longer effective without the presence of oxygen interstitials.

One approach to increase the Ge content without changing the width of the Si_{0.85}Ge_{0.15} nanopillars is to maintain the width constant, in this case at 200 nm (Figure 3) and increase the

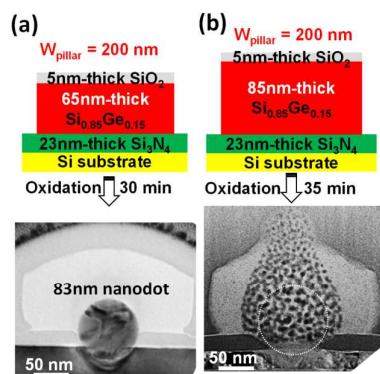


Figure 3 Pillar thickness-dependent morphological and migrational behavior of Ge dot/nanocrystallites formed from thermal oxidation of 200nm-wide Si_{0.85}Ge_{0.15} nanopillars at 900°C in an H₂O ambient. In this case oxygen interstitial flow is not restricted due to the narrower width (200nm) of the Si_{0.85}Ge_{0.15} nanopillars. However, because the Ge content is increased due to the increased thickness of the nanopillars, (a) single, large, spherical Ge nanodots are formed per pillar. Increased Ge nanodot size comes at a cost: Due to their larger surface area for reaction these Ge nanodots rapidly penetrate the Si₃N₄ buffer layer and upon encountering the Si substrate, (b), explode¹¹ when the interstitial Si flux becomes extremely high

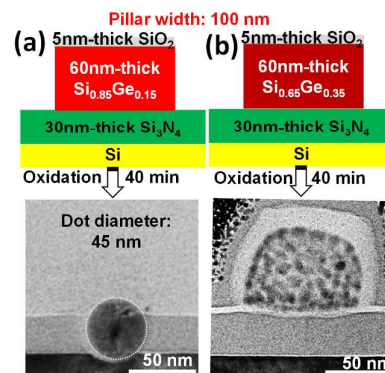


Figure 4 Ge content-dependent morphology and migration of Ge dots/nanocrystals formed after Si_{0.85}Ge_{0.15} and Si_{0.65}Ge_{0.35} nanopillars of similar 100nm width and 60nm thickness are thermally oxidized. The higher Ge content in the Si_{0.65}Ge_{0.35} nanopillars (b) suppresses the flux of oxygen interstitials and consequently the Ge-catalyzed local oxidation of the underlying, Si₃N₄ buffer layer. Hence, Ostwald Ripening of the Ge nanocrystallite clusters does not occur in the higher Ge content case, nor does the Ge migrate into the Si₃N₄ buffer layer as seen for the (a) Si_{0.85}Ge_{0.15} nanopillar case.

height of the nanopillars instead. In this way, we ensure that the lateral flux of oxygen interstitials to the underlying Si₃N₄ buffer layer is not restricted, and the catalytic oxidation of the Si₃N₄ buffer layer can be allowed to proceed. Indeed, in this case, we have observed that large Ge nanodots are formed (Figure 3a). Because of their large reaction surface area, these nanodots are able to migrate rapidly through the Si₃N₄ buffer layer and encounter the Si substrate underneath. Once they have penetrated the Si substrate, the massive increase in Si interstitials¹¹ causes these very large Ge nanodots to explode (Figures 3(b)) via the defect decoration/oxidation mechanism described above.

The combined experimental observations from Figure 2 and 3 reveal that the flux of external oxygen interstitials is a critical component of the combined Ge, Si and oxygen interstitial-enabled Ostwald Ripening and migration process. The lack of oxygen interstitials in proximity of the Ge/Si₃N₄ interface retards the occurrence of the destruction and construction processes for the SiO₂ surrounding the Ge nanocrystallite cluster. Hence, although no coalescence and migration were observed for the case of the wider, high Ge-content nanopillars, both coalescence and migration were restored for the narrower, similar high Ge-content nanopillars.

Further support for the influence of oxygen interstitials in these symbiotic processes is provided by another experiment (Figure 4) in which the Ge content of the nanopillars was increased by changing the Ge mole fraction in the poly-SiGe alloy from Si_{0.85}Ge_{0.15} to Si_{0.65}Ge_{0.35} for nanopillars with dimensions which promoted coalescence and migration in the former case, i.e. width (100nm) and height (60nm). For the case of the poly-Si_{0.65}Ge_{0.35} nanopillars the higher Ge content impedes the flow of oxygen interstitials, effectively blocking the catalytic

oxidation of the Si_3N_4 buffer layer, and consequently also reducing Ostwald Ripening and migration of the Ge nanocrystallite clusters.

For Si oxidation, molecular oxygen O_2 , rather than monoatomic oxygen, has been identified as the major oxidant species that permeates or diffuses through the growing SiO_2 layer. O_2 does not dissociate until it reaches the reaction interface between the SiO_2 and Si substrate.^{19,20,21} The temperature-dependent diffusion coefficient for oxygen interstitials in SiO_2 is $D(\text{O}_2 \text{ in } \text{SiO}_2) = 2 \times 10^{-9} \exp(-1.3\text{eV}/k_B T)$,²² suggesting that at 900°C , the diffusion coefficient of molecular O_2 in SiO_2 is therefore $5.3 \times 10^{-15} \text{ cm}^2/\text{sec}$. Estimated lateral profiles of oxygen interstitial concentrations $C(x) = C_S \exp(-x^2/L_D^2)$, where C_S is the external oxygen concentration at the surface of the nanopillar and L_D denotes the diffusion length ($L_D = 2 \times (Dt)^{0.5}$), along the radial direction (x -axis) of the oxidized nanopillars are plotted right below the corresponding TEM micrographs in Figure 2. These molecular concentration profiles help us to understand the influence (or lack thereof) of oxygen concentration on the Ostwald Ripening and migration of the Ge nanocrystallites. A value of $5.5 \times 10^{18} \text{ cm}^{-3}$ is extracted for the pre-factor C_S from the quadratic reaction rate constant (B) measured experimentally for poly- $\text{Si}_{0.85}\text{Ge}_{0.15}$ oxidized at 900°C in an H_2O ambient (Figure 5). In this case, the relationship between the oxide thickness (d_{ox}) and oxidation time (t) is described well by the Deal-Grove parabolic model²³ of $t = d_{ox}^2/B + d_{ox}(B/A) = d_{ox}^2/658.1545 + d_{ox}/74.81$, where A and B describe the properties of the reaction and the oxide layer, respectively. The parameter B is given by $B = 2D_{\text{SiO}_2}C_S/N_i$, where D_{SiO_2} is the diffusion coefficient of oxygen molecules in SiO_2 and N_i denotes the number of oxygen interstitials/unit volume needed to produce a unit volume of the oxide for thermal oxidation.²⁴ It is clear to see that a high flux of oxygen, in excess of $\sim 3\text{--}4 \times 10^{17} \text{ cm}^{-3}$, diffusing through the newly-formed oxide completes the conversion of the Si content of the original $\text{Si}_{0.85}\text{Ge}_{0.15}$ pillar into SiO_2 . Upon “contact” with the

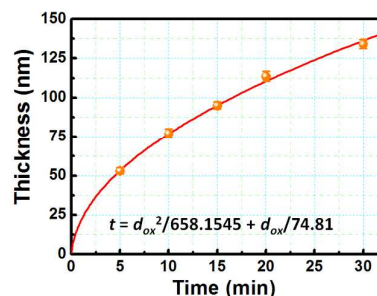


Figure 5 Experimentally-observed thermal oxidation kinetics of poly- $\text{Si}_{0.85}\text{Ge}_{0.15}$ at 900°C in an H_2O ambient. The parabolic behavior follows the Deal-Grove model of $t = d_{ox}^2/B + d_{ox}(B/A) = d_{ox}^2/658.1545 + d_{ox}/74.81$ where t and d_{ox} are in the units of min and nm. An external oxygen concentration at the surface of the nano-pillar (C_S) of $5 \times 10^{18} \text{ cm}^{-3}$ is extracted from the quadratic reaction rate constant (B) that is given as $B = 2D_{\text{SiO}_2}C_S/N_i$.

residual, dense cluster of Ge nanocrystallites, however, the oxygen concentration is significantly reduced because of the Ge's low affinity for oxygen and the low segregation coefficient of oxygen in Ge.²⁵ It has been reported that in order to obtain Ge with high oxygen concentrations, i.e., $>10^{16} \text{ cm}^{-3}$, it is necessary to dope the Ge crystal deliberately, for instance by ion implantation. For the case of the sparse clusters of Ge nanocrystallites (Figure 2(a)), the oxygen interstitial concentrations within the oxide ($>10^{17} \text{ cm}^{-3}$) are sufficient for enabling the Ge-induced, catalytically enhanced local oxidation of the Si_3N_4 buffer layer. This Ge-catalyzed oxidation of the Si_3N_4 buffer layer is suppressed for wide, dense clusters of Ge nanocrystallites as evidenced by only a slight “dent” in the underlying Si_3N_4 layer underneath the cluster of Ge nanocrystallites formed with nanopillars (Figs. 2(b), 2(c) and 4(b)). The oxygen interstitial-induced “chain reaction” is

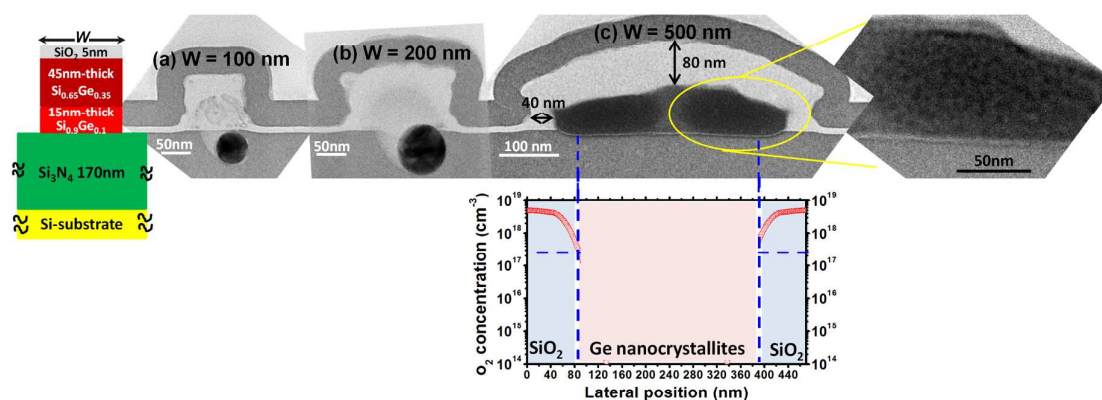


Figure 6 “Designer” nanopillar consisting of a $\text{Si}_{0.65}\text{Ge}_{0.35}/\text{Si}_{0.9}\text{Ge}_{0.1}$ double layer partially overcomes the limitation of oxygen interstitial access to the underlying Si_3N_4 buffer layer. The lower Ge content $\text{Si}_{0.9}\text{Ge}_{0.1}$ layer forms an oxide with a sparse distribution of Ge nanocrystallites following thermal oxidation of the poly- $\text{Si}_{0.9}\text{Ge}_{0.1}$ layer at 900°C for 90 min. Oxygen interstitials are now able to access the underlying Si_3N_4 buffer layer through the intermediate oxide layer, facilitating the local, catalytic oxidation of the underlying Si_3N_4 buffer layer by the Ge nanodot as it penetrates the buffer layer (a) and (b). When the nanopillar width is increased to 500 nm, similar behavior as seen in Fig. 2 is observed, whereby the oxygen interstitials are simply unable to penetrate the wider, dense distribution of Ge nanocrystallites, and access the underlying Si_3N_4 buffer layer.

effectively stopped because the reduced oxygen interstitial concentration is not capable of releasing the requisite flux of Si interstitials from the oxidation of the Si_3N_4 buffer layer, which in turn cannot promote the growth and movement of the Ge nanocrystallites. Hence the Ge nanocrystallite clusters remain static within the oxidized pillar even they are in direct contact with the underlying buffer Si_3N_4 layer.

Armed with the understanding derived from the above results, we are now able to control the access and concentration of oxygen interstitials to the surface of the Si_3N_4 buffer layer through various strategies. Two such strategies include (a) the use of graded-Ge concentration, composite $\text{Si}_{1-x}\text{Ge}_x$ nanopillars or (b) the insertion of a low-Ge content $\text{Si}_{1-y}\text{Ge}_y$ layer between the high-Ge content $\text{Si}_{1-x}\text{Ge}_x$ pillar and the Si_3N_4 buffer layer. The latter strategy exemplified in Figure 6 consists of a $\text{Si}_{0.65}\text{Ge}_{0.35}/\text{Si}_{0.9}\text{Ge}_{0.1}$ double layer that is grown and lithographically patterned over the underlying Si_3N_4 buffer layer. For this “designer” structure, 100–200nm-wide nanopillars no longer restrict the growth and movement of the high-Ge content nanocrystallites into the underlying Si_3N_4 buffer layer. As expected, the lower Ge-content $\text{Si}_{0.9}\text{Ge}_{0.1}$ layer forms an oxide layer with a sparse Ge nanocrystallite distribution following thermal oxidation. Oxygen interstitials are now able to access the underlying Si_3N_4 buffer layer, facilitating the local, catalytic oxidation of buffer Si_3N_4 by the Ge nanodot as it penetrates the buffer layer (Figure 6(a) and (b)). When the nanopillar width is increased to 500 nm however, similar behavior as seen in Figure 2(c), is observed, the oxygen interstitials are simply unable to penetrate the wider, dense distribution of Ge nanocrystallites and promote their growth and migration.

Conclusions

In conclusion, we have observed a unique and interesting symbiotic “chain reaction” promoted by the presence of oxygen interstitials during the high-temperature thermal oxidation of poly-SiGe nanopillars. We have shown that Ge nanocrystallite growth and migration within the SiGe nanopillars is highly sensitive to the concentration of oxygen interstitials at the Ge nanocrystallites/buffer Si_3N_4 interface. A range of different morphologies are observed for the Ge nanocrystallites that are directly attributable to the influence of oxygen interstitial concentration. For Ge nanocrystallites generated from narrow, low Ge-content SiGe nano-pillars, oxygen interstitials are able to diffuse through the oxide containing these sparse Ge nanocrystallite distributions, and initiate the chain-reaction, i.e. the generation and migration of Si interstitials consequently the generation and migration of Ge interstitials, effectively activating the coalescence of the Ge nanocrystallites and their concurrent migration toward the underlying Si_3N_4 buffer layer, the source of Si interstitials. Ostwald ripening and migration, however, does not occur for high-density Ge nanocrystallites generated either from large dimension (width/height) or high Ge-content SiGe nano-pillars, because oxygen interstitials are unable to penetrate dense Ge nanocrystallite clusters, possibly contained with unoxidized SiGe matrices, to access the buffer Si_3N_4 interface. The low concentration of oxygen interstitials within the high-density Ge clusters retards the Ge-catalyzed oxidation of the Si_3N_4 and consequently stops the ripening and migration of the Ge

nanocrystallites. Effective strategies for controlling the oxygen interstitial flux include the use of graded Ge-content poly-SiGe layers or the use of multi-layer stacks of low Ge-content SiGe layers sandwiched between high Ge-content SiGe layers and the buffer Si_3N_4 . We envisage further scientific exploration of this unique phenomenon and the demonstration of new device geometries with Ge QDs buried within various Si containing layers.

It is also interesting to note that this unique phenomenon falls within a so-called “Goldilocks” combination of a specific range of nano-pillar dimensions, oxidation temperature range and range of spatial separations between the Ge nanocrystallite clusters and the source of Si interstitials, namely the Si_3N_4 buffer layer. These are the exclusive conditions which allowed nature to reveal the above, fascinating interplay between O_2 , Si and Ge interstitials and thereby set the foundation for a deeper understanding of the roles of these interstitials. Such insights have eluded previous workers^{26,27} who, unfortunately, reached erroneous conclusions, even suggesting in one instance²⁷ that slow oxidation is the result of Ge suppressing Si interstitials!

Acknowledgements

This work was supported by the Ministry of Science and Technology of Taiwan, Republic of China. (MOST-102-2221-E-009-195-MY3) as well as by the Asian Office of Aerospace Research and Development under contract no FA 2386-15-1-4025.

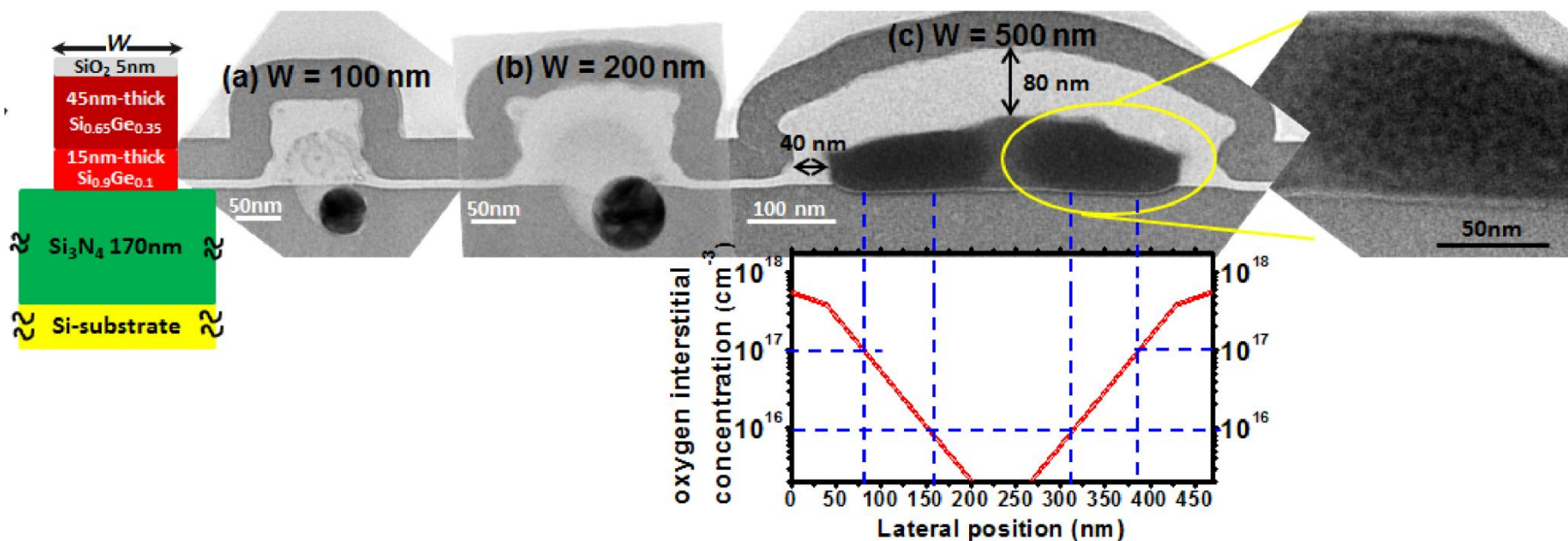
Notes and references

- 1 L. Tsybeskov and D. J. Lockwood, *Proc. IEEE*, 2009, **97**, 1284
- 2 K. L. Wang, D. Cha, J. Liu and C. Chen, *Proc. IEEE*, 2007, **95**, 1866
- 3 Y. Tu and J. Tersoff, *Phys. Rev. Lett.*, 2007, **98**, 096103
- 4 M. Brehm, M. Grydlik, F. Schaffler and O. G. Schmidt, *Microelectronic Engineering*, 2014, **125**, 22
- 5 T. Stoica and E. Sutter, *Nanotechnology*, 2006, **17**, 4912
- 6 E. Sutter, F. Camino and P. Sutter, *Appl. Phys. Lett.*, 2009, **94**, 083109
- 7 Q. Li, S. M. Han, S. R. Brueck, S. Hersee, Y. B. Jiang and H. Xu, *Appl. Phys. Lett.*, 2003, **83**, 5032
- 8 Grydlik M, Langer G, Fromherz T, Schaffler F, Brehm M 2013 *Nanotechnology* 24, 105601.
- 9 F. Liu, A. H. Li, M. G. Lagally, *Phys. Rev. Lett.*, 2001, **87**, 126103
- 10 M. H. Kuo, C. C. Wang, W. T. Lai, T. George and P. W. Li, *Appl. Phys. Lett.*, 2012, **101**, 223107
- 11 C. C. Wang, P. H. Liao, M. H. Kuo, T. George and P. W. Li, *Nanoscale Res. Lett.*, 2013, **8**, 192
- 12 K. H. Chen, C. C. Wang, T. George and P. W. Li, *Nanoscale Res. Lett.*, 2014, **9**, 339
- 13 K. H. Chen, C. C. Wang, T. George and P. W. Li, *Appl. Phys. Lett.*, 2014, **105**, 122102
- 14 C. Y. Chien, Y. R. Chang, R. N. Chang, M. S. Lee, W. Y. Chen, T. M. Hsu and P. W. Li, *Nanotechnology*, 2010, **21**, 505201
- 15 W. Z. Ostwald, *Phys. Chem.*, 1900, **34**, 495
- 16 D. Starodub, E. P. Husev, E. Garfunkel and T. Gustafsson, *Surf. Rev. Lett.*, 1999, **6**, 45
- 17 A. A. Stekolnikov and F. Bechstedt, *Phys. Rev. B*, 2005, **72**, 125326

ARTICLE

CrystEngComm

- 18 P. H. Liao, T. C. Hsu, K. H. Chen, T. H. Cheng, T. M. Hsu, C. C. Wang, T. George and P. W. Li, *Appl. Phys. Letts.*, 2014, **105**, 172106.
- 19 L. Tsetseris and S. T. Pantelies, *Phys. Rev. Lett.*, 2006 **97**, 11601
- 20 M. A. Lamkin and F. L. Riley, *J. European Ceramic Soc.*, 1992 **10**, 347
- 21 R. H. Doremus, *J. Phys. Chem.*, 1976 **80**, 1773
- 22 E. L. Williams, *J. Am. Ceram. Soc.*, 1965 **4**, 190
- 23 B. E. Deal and A. S. Grove, *J. Appl. Phys.*, 1965, **36**, 3770
- 24 C. Claeys and E. Simoen, *Germanium-based Technologies: From Materials to Devices*, Chap. 4, Elsevier BV, Oxford, 2007
- 25 S. Wolf and R. N. Tauber, *Silicon Processing for the VLSI Era* vol. 1, Chap. 7, Lattice Press, California, 1986
- 26 J. Eugene, F. K. LeGoues, V. P. Kesan, S. S. Iyer and F. M. d'Heurle, *Appl. Phys. Lett.*, 1991, **59**, 78
- 27 F. G. LeGoues, R. Rosenberg and B. S. Meyerson, *Appl. Phys. Lett.*, 1989, **54**, 644



We report an unusual “symbiotic” chain reaction promoted by the presence of oxygen interstitials acting in concert with Ge and Si interstitials, inducing morphology changes and autonomous migration of Ge nanocrystallites within $\text{SiO}_2/\text{Si}_3\text{N}_4$ layers. In combination with Si and Ge interstitials, oxygen interstitials activate the coalescence of sparsely-distributed Ge nanocrystallites and concurrently their migration towards the source of Si interstitials. These symbiotic effects are “tunable” by increasing the Ge content of the SiGe nano-pillars.